



# Newly Acquired Gravity Data in Support of the GeoNetGNSS CORS Network in Northern Greece

D. A. Natsiopoulos, E. G. Mamagiannou, A. Triantafyllou, E. A. Tzanou, G. S. Vergos, I. N. Tziavos, D. Ramnalis, and V. Polychronos

## Abstract

The main purpose of the GeoNetGNSS project, funded by the European Union and National Funds through the Region of Central Macedonia (RCM), is to establish a dense network of Continuously Operating Reference Stations (CORS) in northern Greece to support geodetic, surveying, engineering, and mapping applications. A regional, high-accuracy and high-resolution gravimetric geoid model is essential for the accurate determination of physical heights from CORS so as to transform the geometric heights into orthometric ones. In that frame and given the geological complexity and topographic peculiarities of the region, gravity campaigns have been designed and carried out around the newly established CORS stations to densify the already available land gravity database. The observations have been carried out employing the GravLab CG5 relative gravity meter and have been referred to GRS80/IGSN71, relative to the absolute gravity stations established by GravLab at the AUTH premises using the A10 (#027) absolute gravity meter. Moreover, dual-frequency GNSS receivers in network real time kinematic (NRTK) mode were used for orthometric height determination. This work also leverages a database of previous gravity measurements to ensure the data coverage for the region. The XGM2019e Global Geopotential Model (GGM) has been used to model the low frequencies. Moreover, as the development of the geoid model is based on the Remove-Compute-Restore (RCR) technique and the Least Squares Collocation (LSC), the topographic corrections were calculated by the spectral Residual Terrain Model (RTM) method. In this work, the gravity anomalies derived from terrestrial gravity observations over the wider region of Central Macedonia are analyzed and compared with gravity anomalies derived from the XGM2016e GGM. The evaluation of the terrestrial gravity data was performed over six separate traverses, at various heights, in order to investigate the effect of height on the measurements. This technique allows for the comparison of the magnitude of gravity anomalies and the correlation with height, providing a more comprehensive understanding of the region's gravitational field and possible improvement with the newly acquired data.

## Keywords

CG5 · Gravity field · Relative gravity · Terrestrial gravity · XGM2016e

D. A. Natsiopoulos · E. G. Mamagiannou · A. Triantafyllou · G. S. Vergos (✉) · I. N. Tziavos  
Laboratory for Gravity Field Research and Applications (GravLab),  
Department of Geodesy and Surveying, Aristotle University of  
Thessaloniki, Thessaloniki, Greece  
e-mail: [vergos@topo.auth.gr](mailto:vergos@topo.auth.gr)

E. A. Tzanou  
Department of Surveying and Geoinformatics Engineering, School of  
Engineering, International Hellenic University, Serres, Greece  
D. Ramnalis · V. Polychronos  
GeoSense PCo, Thessaloniki, Greece

## 1 Introduction

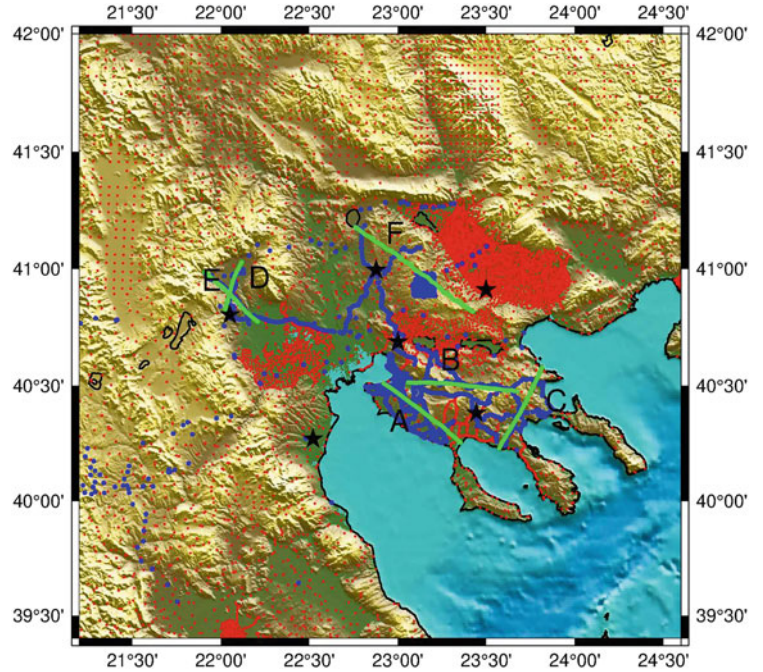
The main goal of the GeoNetGNSS project (GeonetGNSS n.d.) is to establish a dense network of Continuously Operating Reference Stations (CORS) in Northern Greece to support high-accuracy horizontal and vertical position determination for engineering and geodetic applications. The construction of an efficient and cost-effective system to determine physical heights with GPS requires a highly accurate gravimetric geoid model, which is derived from a multitude of gravimetric observations obtained from various sensors and platforms. To achieve this, it is crucial to understand the characteristics of each type of gravity measurement, stemming from historical to recent campaigns, different instrumentation used, etc. This also requires a very good knowledge of the topography in order to determine accurate topographic effects. In this frame, and given both the geological complexity and topographic peculiarities of the area as well as gaps in the existing gravity database, dedicated gravity campaigns have been designed and carried out around the newly established CORS. The aim was to acquire new gravity observations, both around the new CORS and to fill-in areas where the existing free-air gravity anomaly database has voids and gaps (Grigoriadis 2009). The latter have been utilized in the latest calculated geoid models for Greece (Tziavos et al. 2010, 2013). In the frame of the present work, and depending on the gravity data used, two free-air gravity anomaly models are determined. The first one, called original, where only existing data are used, and a second one, called merged, where the original point gravity anomalies are merged with the newly acquired ones. In this paper, we first summarize the collection and post-processing of gravity and GNSS/Leveling data to densify the available land gravity database in Northern Greece and investigate the effect of height on the gravity data, in order to quantify whether the newly acquired data over areas with gaps improve the gravity field representation. Then, as the estimation of the geoid in a next step will be based on the RCR concept, and in order to compute residual free-air gravity anomalies, the XGM2019e GGM (Zingerle et al. 2019) was used as a reference for modeling the low-frequency part of the spectrum. The topographic effects were calculated through a spherical harmonics representation of the Earth's potential and high-resolution residual terrain corrections from a global model (Hirt et al. 2014; Rexer et al. 2018). The such derived residual gravity anomalies are used to predict gravity anomalies using the Least-Squares Collocation (LSC) technique (Sansò and Sideris 2013; Tscherning 2013), based on the analytical covariance functions of the collocation. The LSC was employed to estimate gravity anomalies over six test traverses spanning the entire region, in an effort to evaluate

the improvement brought by including the newly acquired data to the available gravity database.

## 2 Study Area and Gravity Measurements

The Region of Central Macedonia (RCM) is located in northern Greece and bounded by  $39.4^\circ \leq \varphi \leq 42^\circ$  and  $21.2^\circ \leq \lambda \leq 24.6^\circ$  (see Fig. 1). It is mainly a low-land area, but on the other hand some of the highest mountains in Greece like Mount Olympus (to the south), Mount Voras (to the north) and Mount Athos (in the third leg of Chalkidiki peninsula) are situated within its bounds. RCM has an extensive coastline with the characteristic peninsula of Chalkidiki in its central part (see Fig. 1) showing varying topographic and morphological characteristics. These pose significant challenges in the accurate determination of the gravity field and the geoid, as quality data are needed over areas with steep terrain which are succeeded by coastal areas with totally different topographic characteristics. Several measurement campaigns were initiated to collect gravity data at various selected sites along the RCM region, aiming to gather high precision gravimetric data and fill-in the gaps in the existing database of the Laboratory of Gravity Field Research and Applications (GravLab) of the Aristotle University of Thessaloniki (AUTH). In this study, we use GravLab's Scintex CG-5 relative gravity meter, which is one of the standard instrumentations used in relative campaigns with a standard deviation (std) of measurement less than  $5 \mu\text{Gal}$  and a low drift of the order of  $0.02 \text{ mGal/day}$  (Lederer 2009; Yushkin 2011). Before the start of each measurement campaign, survey parameters, corrections, and filters including Tide Correction, Continuous Tilt Correction, Auto Rejection Filter and Seismic Filter have been set. The terrain correction estimation provided by the software of CG-5 has not been used, as we will model the topographic effects through a spherical harmonics expansion of the topographic potential to degree and order (d/o) 2,190 (Hirt et al. 2014) and estimate high-order residual terrain model effects as it is suggested by (Rexer et al. 2018). The field campaigns were carried out in most cases along the road network of the area under study, collecting gravity measurements at a spatial resolution of 1 km, in order to observe the local variations of the gravity field. The reading time for each occupation was set at 60 s with a 5 s start delay for each observation set. At the absolute gravity stations which have been used at the beginning of each daily campaign, five sets of observations have been taken in order to increase the accuracy of the mean observation. In all relative campaigns we have used as reference point the AUTH1 absolute gravity benchmark (BM)

**Fig. 1** Distribution of original (red dots) and new (blue dots) gravity data and the locations of the new CORS stations (black stars) and test traverses (green lines)



located at the premises of the University campus. This BM has been established by GravLab using the Micro-Lacoste A10 (#027) absolute gravity meter with a gravity value of  $980,276,178.42 \pm 10.05 \mu\text{Gal}$ .

In the frame of the gravity campaigns, 2,156 new gravity densification points have been established with their position determined through geodetic-grade GNSS receivers measuring in Network Real Time Kinematic (NRTK) mode. For each new station, 10 epochs of 1 Hz GNSS observations have been collected employing the Virtual Reference Station (VRS) mode and acquiring differential corrections from the Hellenic Positioning Service (HEPOS). These data were merged with the already available 13,961 land free-air gravity anomalies (Grigoriadis 2009) resulting in a total number of 16,117 irregularly distributed observations in the area under study. Figure 1 depicts the old (red) and newly acquired (blue) gravity observations along with the newly established CORS (black stars), while the six validation traverses are shown in green and are numbered from A to F. The six traverses are located on regions that exhibit diverse topographic and land/sea characteristics as well as over regions with sparse original gravity data. Three traverses are situated in the southern part of RCM close to Chalkidiki, one in the west, one in the center, and one in the east part of the test area (traverse A–C respectively), two in the northwest part of RCM (traverse D and E) and one in the north-central part (traverse F). It should be mentioned that the collection of gravity data is a work still in progress, as we need to fill-in observations for the two westernmost stations in Katerini (south-west star in Fig. 1) and Edessa (north-west star in Fig. 1). Especially, the station over Katerini is in close proximity

with Mt. Olympus and the Olympus mountain range, where very few observations exist in our historical database.

### 3 Relative Gravity Data Processing

In the frame of each measurement campaign, and during each occupation, the quality of the instrument gravity readings is monitored continuously in order to inspect the reading accuracy. In the event that measurements were degraded due to anthropogenic or weather-related factors (e.g. heavy traffic, wind, pedestrians walking by, etc.), then they were immediately discarded and the measurements were repeated. The observations quality of each 60 s measurement was ensured by setting a threshold of  $20 \mu\text{Gal}$  for the observation standard deviation, i.e., the instrument accuracy which is the mean of the variances of each 1 s individual observation. In that sense, if the precision of the measurement exceed the  $20 \mu\text{Gal}$  level, then the observation was repeated. All campaigns started from the aforementioned AUTH1 absolute gravity station and ended each day at the same station. Therefore, each daily misclosure at AUTH1, as the difference of the observations at the reference station at the beginning and the end of each daily campaign, has been treated as an additional drift correction. From the determined gravity value  $g$  for each station, the normal gravity in GRS80 ( $\gamma_0$ ) is subtracted and finally the free-air gravity anomalies ( $\Delta g_F$ ) are derived using the free-air reduction ( $\delta g_F$ ):

$$\Delta g_F = g - \gamma_0 + \delta g_F. \quad (1)$$

**Table 1** Statistics of the local free-air gravity anomaly field and their residuals. Units: [mGal]

	Max	Min	Mean	Std
$\Delta g_f$ merged data	-137.985	258.979	17.022	$\pm 53.172$
$\Delta g_{XGM}$ merged data	-126.789	212.762	22.213	$\pm 49.116$
$\Delta g_{TOPO}$ merged data	-108.448	81.144	-5.454	$\pm 16.542$
$\Delta g_{f\ res}$ merged data	-63.302	116.492	0.263	$\pm 13.722$
$\Delta g_f$ orig. data	-137.985	258.979	11.109	$\pm 53.632$
$\Delta g_{XGM}$ orig. data	-126.789	212.762	17.156	$\pm 49.835$
$\Delta g_{TOPO}$ orig. data	-108.448	81.144	-5.418	$\pm 17.301$
$\Delta g_{f\ res}$ orig. data	-63.302	113.095	-0.629	$\pm 13.012$

The main objective of the GeoNetGNSS project is to finally determine a high resolution and accuracy gravimetric and hybrid geoid model through the application of the RCR technique (Barzaghi et al. 2019; Tscherning and Forsberg 1987). This involves the removal of both the long and short wavelengths of the gravity field spectrum from the input data. XGM2019e complete to d/o 2,190 (Zingerle et al. 2019) has been selected as a reference to model the long-wavelength component of the spectrum (Forsberg and Tscherning 2008), while the topographic effects are calculated through a spherical harmonics expansion of the Earth's potential and the residual terrain correction (RTC) from a global model (Hirt et al. 2014; Rexer et al. 2018). Thus, residual free-air gravity anomalies can be calculated as:

$$\Delta g_{f\ res} = \Delta g_f - \Delta g_{GGM} - \Delta g_{topo}, \quad (2)$$

where,  $\Delta g_{f\ res}$  denote the residual gravity anomalies,  $\Delta g_f$  the available free-air gravity anomalies,  $\Delta g_{GGM}$  the contribution of the GGM and  $\Delta g_{topo}$  the contribution of the topography. Table 1, tabulates the corresponding statistics for both the original and merged gravity datasets. The merged residual free-air gravity anomalies show a higher standard deviation by 0.7 mGal and a smaller mean by 0.4 mGal compared with the original free-air gravity anomalies.

In order to evaluate the influence of the recent gravity data in the representation of the Earth's gravity field over the study area, LSC has been used to predict free-air gravity anomalies from the original and merged datasets to the six aforementioned traverses. LSC is frequently used in physical geodesy to interpolate and estimate gravity-related quantities with the challenge being to model appropriately the analytical covariance function to be used. Two different empirical

covariance functions have been estimated (see Fig. 2), one for the merged gravity data set and one for the original gravity data set, while in both cases the analytical model was that of Tscherning and Rapp (1974). The empirical covariance functions have been estimated with an in-house developed software in Matlab © while the analytical model has been fitted using the covfit module of the Gravsoft gravity field modeling software (Forsberg and Tscherning 2008).

As it can be seen in Fig. 2, the merged residual gravity anomalies present higher power compared to the original ones, which can be attributed to the better representation of the local gravity variations in the area under study. The merged data has a correlation length (denoted by  $\xi$  in Fig. 2) that is nearly half that of the original datasets (6.2 km compared to 12.78 km), thus indicating that the merged dataset presents a smoother signal of the local gravity field after the removal of the XGM2019e and RTM contributions. The so-determined models of analytical covariance functions have been used to estimate, from the irregularly distributed original and merged gravity data, residual gravity anomalies at the test traverses, while then the effects of the topography and that of the GGM were restored. The prediction has been carried out both over regions that exhibit diverse topographical and land/sea attributes and regions with sparse original gravity data. For all six test traverses mentioned above, the differences among the original, merged, and XGM2019e gravity anomaly data were computed, with their statistics tabulated in Table 2 and their differences depicted in Fig. 3, along with their corresponding statistics presented in Table 3. It should be noted that the original, historic, gravity data have been incorporated in the development of EGM2008 (Pavlis et al. 2012), hence this should influence the statistics achieved. The analysis of their differences indicates that the merged dataset exhibits a stronger representation of the real gravity signal than the original dataset, especially in traverse A between points 25–35, in traverse B between points 30–35, and in traverse F between points 30–40. It is evident that the merged dataset (represented by the blue dashed line) provides a significantly better representation of local gravity variations in the study area for these specific points, introducing higher frequencies compared to the old dataset. In most cases, the original database provides a smaller standard deviation to XGM2019e, but this is something expected, as XGM2019e is based on the EGM2008 terrestrial dataset to a resolution of  $0.25 \times 0.25^\circ$  (corresponding to d/o 720). Hence, both the original gravity dataset and XGM2019e do

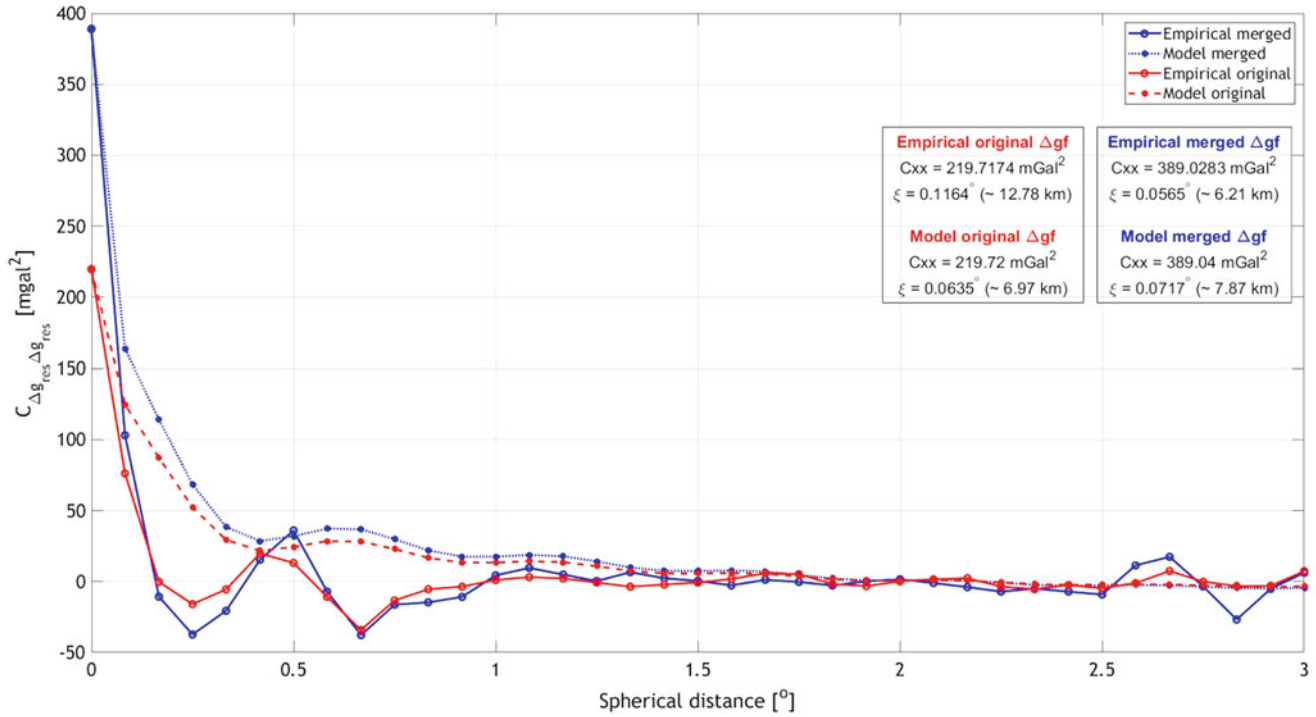


**Fig. 2** Empirical covariance functions of the residual gravity anomalies and fitted analytical models for the original and merged datasets (where  $\xi$  in the figure text denotes the correlation length)

**Table 2** Statistics of the differences between the original, merged and XGM2019e gravity anomalies for each of the traverses studied. Units: [mGal]

Traverse	Differences to XGM2019e	Max	Min	Mean	Std
A	Original	20.242	-24.614	-0.496	11.168
	Merged	19.788	-24.011	-2.250	13.285
B	Original	40.401	-24.114	0.710	15.248
	Merged	44.208	-22.841	-1.420	16.777
C	Original	41.223	-20.046	5.366	13.310
	Merged	53.037	-23.928	2.748	15.858
D	Original	9.747	-21.661	-5.123	10.598
	Merged	6.853	-26.521	-7.876	10.481
E	Original	14.260	-49.964	-6.309	15.658
	Merged	12.372	-55.989	-8.783	16.873
F	Original	36.748	-16.783	3.871	11.654
	Merged	36.503	-21.294	3.123	13.366

not manage to represent some fine details in the local gravity features of the area, given the undersampling of original dataset, especially over rugged terrain. Of course, this is not a problem over areas of lower terrain like traverse D (see after gravity point 8).

Additional insights can be derived by estimating the correlation coefficient between free-air gravity anomalies and height, as, primarily, the higher frequencies depicted by the merged dataset should lead to improved correlation

coefficients. This has been done for both the two local gravity anomaly datasets and XGM2019e, the latter setting the threshold for the global models. Table 3 summarizes the correlation coefficients estimated, where it can be seen that in all cases the new merged dataset provides a, slightly or significantly, higher correlation. The results indicate that the incorporation of the new gravity data yielded a significantly enhanced correlation throughout all regions, with a notable increase of 0.2 (37.5%) observed in the western part of Chalkidiki (traverse A), where very few observations existed in the original database, while now extensive data have been collected. A slightly smaller improvement is found over traverse B in the central part of Chalkidiki (from 0.78 to 0.84 or 13.5%), which is expected as in that region the original database contains observations. Over traverse C the improvement reaches 26.4%, 3% over traverse D, 4% over traverse E and 3.6% over traverse F. XGM2019e presents in all cases slightly lower correlation with topography but very close to the original dataset, which is an indication of the high-quality of the GGM. This is something expected as most of the historical terrestrial gravity data in Greece have been used in the development of EGM2008 and hence in XGM2019e as the latter incorporates the terrestrial gravity data of EGM2008 to a resolution of  $0.25 \times 0.25^\circ$ , which corresponds to spherical harmonics degree 720. On the other hand, especially over traverse A in the western part of Chalkidiki, XGM2019e shows a correlation with topography

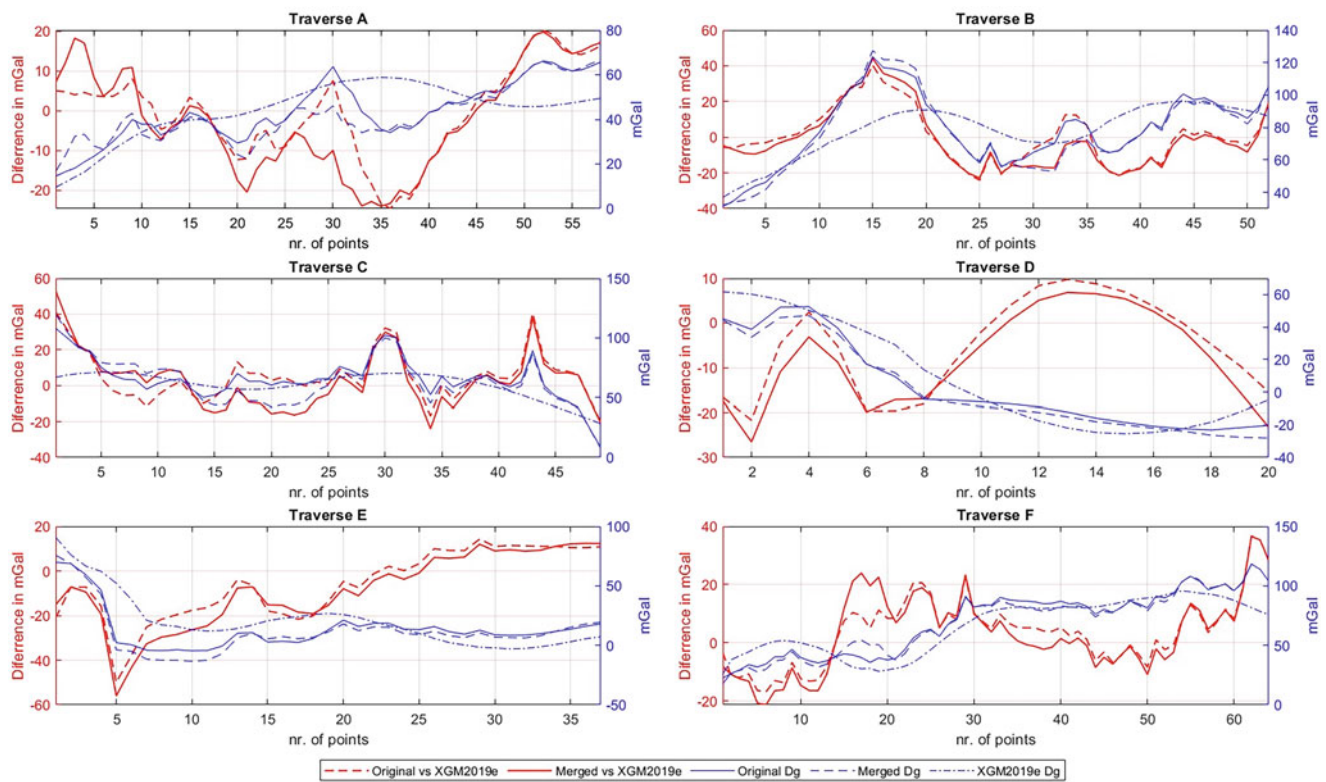


**Fig. 3** Original, merged and XGM2019e gravity anomalies, and their differences, along the traverses

**Table 3** Correlation between gravity anomalies and elevation

TRAVERSE	Original data	Merged data	XGM2019e
A	0.557	0.766	0.159
B	0.784	0.844	0.803
C	0.486	0.614	0.452
D	0.936	0.962	0.860
E	0.845	0.888	0.851
F	0.831	0.857	0.944

at the 0.159 level only, while the original dataset is at the 0.557. This is quite peculiar and might be attributed to some of the old data not being used in its development, but it is still an issue that requires further investigation. What is evident though is that especially over that part of the area under study, where dense new observations have been collected, the improvement is significant. Therefore, taking more gravity measurements and filling the gaps in existing databases over a region, can help to better capture and understand the variations of the underlying topography, model the underlying mass distribution and thus derive a more precise representation of the gravity field and the geoid.

## 4 Conclusions

The GeoNetGNSS project aims to establish a dense network of CORS in Northern Greece for the construction of an accurate gravimetric geoid model. To achieve this, gravity campaigns have been designed and carried out around the newly established CORS, and these data were combined with already available free-air gravity anomalies resulting in a total number of 16,117 irregularly distributed point values. Details on the study area, measurement equipment, and processing of the data, including the calculation of free-air gravity anomalies have been given. After removing both the long and short wavelengths of the gravity field spectrum least, the LSC method was used to predict over six separate traverses, towards the evaluation of the terrestrial gravity data. By incorporating the new denser gravity dataset, the correlation in all regions improved significantly, particularly in the western part of Chalkidiki, where few gravity observations were available in the previously available dataset. This area showed a noticeable increase of 0.2 in the correlation coefficient which is an improvement by 37.5%. The current

campaigns will be enhanced with additional gravity acquisitions over the western part of the area under study where some dominant topographic features, like Mount Olympus are found. It is expected that the recently acquired datasets will substantially enhance the accuracy in the gravimetric and hybrid geoid models to be determined. The latter are to serve to the ultimate goal of the GeoNetGNSS project, which is to support accurate GNSS-based orthometric height determination over RCM.

**Acknowledgements** This research was carried out as part of the project “GeoNetGNSS” (Project code: KMP6-0071139) under the framework of the Action “Investment Plans of Innovation” of the Operational Program “Central Macedonia 2014-2020”, that is co-funded by the European Regional Development Fund and Greece.

## References

- Barzaghi R, Carrion D, Vergos GS, Tziavos IN, Grigoriadis VN, Natsiopoulou DA, Bruinsma S, Reinquin F, Seoane L, Bonvalot S, Lequentrec-Lalancette MF, Salaün C, Andersen O, Knudsen P, Abulaitijiang A, Rio MH (2019) GEOMED2: high-resolution geoid of the Mediterranean. In: Freymueller J, Sánchez L (eds) International Association of Geodesy Symposia. pp 43–50. [https://doi.org/10.1007/1345\\_2018\\_33](https://doi.org/10.1007/1345_2018_33)
- Forsberg R, Tscherning CC (2008) An overview manual for the GRAVSOFT geodetic gravity field modelling programs. Contract report for JUPEM, 2nd edn. - References - Scientific Research Publishing
- GeonetGNSS (n.d.) GeonetGNSS [WWW Document]
- Grigoriadis V (2009) Geodetic and geophysical approximation of the Earth's gravity field and applications in the Hellenic area, PhD Thesis, Aristotle University of Thessaloniki (in Greek)
- Hirt C, Kuhn M, Claessens S, Pail R, Seitz K, Gruber T (2014) Study of the earth's short-scale gravity field using the ERTM2160 gravity model. *Comput Geosci* 73:71–80. <https://doi.org/10.1016/j.cageo.2014.09.001>
- Lederer M (2009) Accuracy of the relative gravity measurement. *Acta Geodyn Geomater* 6:383–390
- Pavlis NK, Holmes SA, Kenyon SC, Factor JK (2012) The development and evaluation of the Earth Gravitational Model 2008 (EGM2008). *J Geophys Res Solid Earth* 117. <https://doi.org/10.1029/2011JB008916>
- Rexer M, Hirt C, Bucha B, Holmes S (2018) Solution to the spectral filter problem of residual terrain modelling (RTM). *J Geod* 92:675–690. <https://doi.org/10.1007/S00190-017-1086-Y/FIGURES/12>
- Sansò F, Sideris MG (2013) The local modelling of the gravity field by collocation. *Lecture notes in earth system sciences*, vol 110, pp 203–258. [https://doi.org/10.1007/978-3-540-74700-0\\_5/COVER](https://doi.org/10.1007/978-3-540-74700-0_5/COVER)
- Tscherning CC (2013) Geoid determination by 3D least-squares collocation. *Lecture notes in earth system sciences*, vol 110, pp 311–336. [https://doi.org/10.1007/978-3-540-74700-0\\_7/TABLES/6](https://doi.org/10.1007/978-3-540-74700-0_7/TABLES/6)
- Tscherning CC, Forsberg R (1987) Geoid determination in the Nordic countries from gravity and height data. *Bollettino di geodesia e Scienze Affini* 46:21–43
- Tscherning CC, Rapp R (1974) Closed covariance expressions for gravity anomalies, geoid undulations, and deflections of the vertical implied by anomaly degree variance models. Report No 208, pp 1–89
- Tziavos IN, Vergos GS, Grigoriadis VN (2010) Investigation of topographic reductions and aliasing effects on gravity and the geoid over Greece based on various digital terrain models. *Surv Geophys* 31. <https://doi.org/10.1007/s10712-009-9085-z>
- Tziavos IN, Vergos GS, Mertikas SP, Daskalakis A, Grigoriadis VN, Tripolitsiotis A (2013) The contribution of local gravimetric geoid models to the calibration of satellite altimetry data and an outlook of the latest GOCE GGM performance in Gavdos. *Adv Space Res* 51. <https://doi.org/10.1016/j.asr.2012.06.013>
- Yushkin VD (2011) Operating experience with CG5 gravimeters. *Meas Tech* 54:486–489. <https://doi.org/10.1007/S11018-011-9753-5/FIGURES/1>
- Zingerle P, Pail R, Gruber T, Oikonomidou X (2019) The experimental gravity field model XGM2019e. GFZ Data Serv. <https://doi.org/10.5880/ICGEM.2019.007>

**Open Access** This chapter is licensed under the terms of the Creative Commons Attribution 4.0 International License (<http://creativecommons.org/licenses/by/4.0/>), which permits use, sharing, adaptation, distribution and reproduction in any medium or format, as long as you give appropriate credit to the original author(s) and the source, provide a link to the Creative Commons license and indicate if changes were made.

The images or other third party material in this chapter are included in the chapter's Creative Commons license, unless indicated otherwise in a credit line to the material. If material is not included in the chapter's Creative Commons license and your intended use is not permitted by statutory regulation or exceeds the permitted use, you will need to obtain permission directly from the copyright holder.

